Special Issue

Journal of Physical Organic Chemistry

Received: 31 October 2007, Revised: 15 January 2008, Accepted: 18 January 2008, Published online in Wiley InterScience: 21 May 2008

(www.interscience.wiley.com) DOI 10.1002/poc.1346

A chemical understanding for the enhanced hydrogen tunnelling in hydroperoxidation of linoleic acid catalysed by soybean lipoxygenase-1

Monica Barroso[a], Luis G. Arnaut[a] and Sebastião J. Formosinho[a]*

The reaction path of the Interacting-State Model (ISM) is used with the Transition-State Theory (TST) and the semiclassical correction for tunnelling (ISM/scTST) to calculate the rates of H-atom abstraction from C(11) of linoleic acid catalysed by soybean lipoxygenase-1 (SLO), as well as of an analogous uncatalysed reaction in solution. The calculated hydrogen-atom transfer rates, their temperature dependency and kinetic isotope effect (KIE) are in good agreement with the experimental data. ISM/scTST calculations reveal the hypersensitivity of the rate to protein dynamics when the hydrogen bonding to a carbon atom is present in the reaction coordinate. Copyright © 2008 John Wiley & Sons, Ltd.

Keywords: enzyme catalysis; soybean lipoxygenase-1; rate constants; kinetic isotope effect

INTRODUCTION

The hydroperoxidation of linoleic acid catalysed by soybean lipoxygenase-1 (SLO), which is formally the abstraction of a hydrogen atom from the C(11) position of the substrate by the Fe(III)—OH cofactor, exhibits nearly temperature-independent rates and kinetic isotope effects (KIE), which are close to 80 at room temperature.[1] Such large and temperature-independent KIE were recently claimed to be inconsistent with the Transition-State Theory (TST) view of catalysis. The difficulties of TST stimulated the formulation of alternative theories.[2–8] Indeed, this KIE is much higher than that observed in other H-atom abstractions; for example, that of the $H + H_2$ *versus* $H + D_2$ hydrogen (deuterium) transfer is only 9.5 ± 1.4 at 30 °C.[9] The complexity of enzyme catalysis did not dissuade several groups of pursuing more sophisticated versions of TST in the treatment of these systems, to show that tunnelling and recrossing corrections may account for the extreme behaviours sometimes observed.[10–14] The enhanced hydrogen tunnelling of the SLO catalysed reaction lead Klinman and co-workers[15] to propose that the 'optimization of enzymes catalysis entails evolutionary strategies to increase tunnelling for the acceleration of rates'. The experimental test of this hypothesis with other systems did not support its generality.[16]

The intense experimental scrutiny of enzyme catalysis is paralleled by an enormous theoretical and computational effort to contribute to the advancement of this field. The understanding emerging from sophisticated computational approaches is that enzymes are extremely complicated biomolecules both from the structural and the dynamical point of view. The theoretical study of the enzyme catalysis is very demanding and requires a lot of computational time to obtain a quantitative picture of how it works. Still, in many cases, the reaction energy given by QM/MM calculations for a given enzymatic reaction may be wrong by 10 kcal/mol or more, and the kinetic data they provide only carry meaningful information on relative rates. Some of the problems associated with such studies are the need to deal with thousands of atoms, to represent the solvation waters, the multiplicity of binding sites and reaction valleys, many conformations, a huge number of minima and transition state structures, the existence of multiple steps beyond the simplified Michaelis–Menten mechanism, the existence of long-range electrostatic interactions.

We have recently shown that the Intersecting/Interacting-State Model (ISM) associated with semiclassical TST provides a reliable way to calculate absolute rates of elementary chemical reaction, notably hydrogen-atom transfers, proton transfers and methyl transfers,[9,17–20] and offers a chemical understanding of reactivity in polyatomic systems. ISM deals in a compact manner with the chemical bonds that are broken and formed in a chemical reaction, characterizing them by their Morse potentials and equilibrium bond lengths, and associates their interactions along a unidimensional reaction coordinate with the reaction energy and an electronic parameter, the electrophilicity index proposed by Parr to measure the saturation of the electron inflow between interacting atoms.[21] Therefore, ISM uses only a small number of effective parameters, which favours the human 'understanding' of reactive processes. In the present paper, we employ ISM/scTST to account for enhanced tunnelling driven by hydrogen bonding in the reaction path of an enzymatic reaction where extreme

* *Chemistry Department, University of Coimbra, P-3049 Coimbra Codex, Portugal.*
E-mail: sformosinho@qui.uc.pt

a *M. Barroso, L. G. Arnaut, S. J. Formosinho*
Chemistry Department, University of Coimbra, P-3049 Coimbra Codex, Portugal

tunnelling effects are found: the *proton-coupled electron transfer* (PCET) step in the hydroperoxidation of linoleic acid catalysed by SLO.

THEORETICAL METHODOLOGY

ISM/scTST calculations

Rate-determining enzymatic H-atom transfers correspond to the breaking of a C—H bond and the formation, in a synchronous manner, of another bond, typically an O—H or N—H bond. This elementary step can be written as

$$AH + B \xrightarrow{k} A + HB \qquad (I)$$

Along the reaction coordinate for the rate-determining step, there is an increase in the potential energy up to the transition state, and subsequently a decrease. The reaction energy barrier is only controlled by the relative energy of the transition state with respect to the reactants, but in order to properly assess quantum mechanical tunnelling and primary KIE one requires the entire barrier shape. This information can be obtained using the ISM.

ISM is based on three fundamental assumptions. The first one is based on the concept of bond-order conservation along the reaction coordinate, provided by the BEBO model of Johnston and Parr[22]

$$n = n_{HB} = 1 - n_{HA} \qquad (1)$$

where n_{HB} is the bond order of the new bond formed in the products and n_{HA} is the bond order of the bond that is broken in the reactants.

The classical reaction path of ISM is a linear interpolation between the Morse curves of HA and HB along the reaction coordinate

$$V_{cl}(n) = (1-n)V_{HA} + nV_{HB} + n\Delta V^0 \qquad (2)$$

where ΔV^0 is the reaction energy.

The second assumption of ISM is based on the Pauling relation between bond lengths and bond orders,[23] generalized to transitions states

$$\begin{aligned} l^{\ddagger}_{HB} - l_{HB,eq} &= -a'_{sc}\left(l_{HA,eq} + l_{HB,eq}\right)\ln\left(n^{\ddagger}\right) \\ l^{\ddagger}_{HA} - l_{HA,eq} &= -a'_{sc}\left(l_{HA,eq} + l_{HB,eq}\right)\ln\left(1 - n^{\ddagger}\right) \end{aligned} \qquad (3)$$

where a'_{sc} is a 'universal' constant, to relate transition state bond lengths ($l^{\ddagger}$) to the corresponding bond orders ($n^{\ddagger}$) and to the equilibrium bond lengths of reactants and products ($l_{HA,eq}$ and $l_{HB,eq}$). The scaling by $a'_{sc}(l_{HA,eq} + l_{HB,eq})$ reflects the fact that longer bonds will stretch out more from equilibrium to the transition-state configurations than shorter ones, and that two bonds are implicated in the transition state. The value of a'_{sc} was obtained from the bond extension of the $H + H_2$ system,[24] $a'_{sc} = 0.182$.

The last assumption concerns the method to account for the electronic stabilization when A and B—C interact at the transition state, $\{A\cdots B\cdots C\}^{\ddagger}$. The electrophilicity index m proposed by Parr represents the saturation point for electron inflow as the ratio between the negative of the electronic chemical potential, μ_{el}, and the chemical hardness, η_{el}, and is a good measure for the extra electronic stabilization of the transition state:[21]

$$m = \frac{-\mu_{el}}{\eta_{el}} = \frac{I_P + E_A}{I_P - E_A} \qquad (4)$$

where I_P is the ionization potential and E_A is the electron affinity of A or B. It increases with the propensity of the 'ligands' A and C to participate in partial electron transfer with the transition state (low I_P and/or high E_A), but otherwise leads to no stabilization (high I_P and/or low E_A). The electronic saturation further stabilizes the transition state and was introduced in the ISM reaction coordinate through a modification of the reactant and product Morse curves[9,17,18,25,26]

$$\begin{aligned} V_{HA} &= D_{e,HA}\{1 - \exp[\beta_{HA}\Delta l_{HA}/m]\}^2 \\ V_{HB} &= D_{e,HB}\{1 - \exp[\beta_{HB}\Delta l_{HB}/m]\}^2 \end{aligned} \qquad (5)$$

where $D_{e,HA}$ and $D_{e,HB}$ are the electronic dissociation energies, β_{HA} and β_{HB} the spectroscopic constants of the bonds HA and HB.

The maximum along the vibrationally adiabatic path with respect to the reactants, $\Delta V^{\ddagger}_{ad}$, is calculated adding the difference in zero-point energy (ZPE) to the classical energy at each point along the reaction path

$$V_{ad}(n) = V_{cl}(n) + \sum_i \left(\tfrac{1}{2}hc\bar{\nu}_i\right) \qquad (6)$$

where $\bar{\nu}_i$ are the vibration frequencies of the normal modes orthogonal to the reaction coordinate. We estimate the frequencies of the linear triatomic transition state from Wilson's equation with the neglect of the interaction between bending and stretching,[27] using fractional bonds in the $\{A\cdots B\cdots C\}^{\ddagger}$ transition state and a switching function to provide the correct asymptotic limits.[9] The linear relation between symmetric stretching and bending frequencies in triatomic systems is employed to estimate the bending frequency from the symmetric stretching frequency.[9]

The semiclassical TST formulation for a bimolecular rate constant in the gas phase is[26,28]

$$k = \kappa(T)\frac{k_B T}{h}\frac{Q_{\ddagger}}{Q_{AH}Q_B}\exp\left(-\frac{\Delta V^{\ddagger}_{ad}}{RT}\right) \qquad (7)$$

where $\kappa(T)$ is a tunnelling correction, $Q_{\ddagger}$, Q_{AH} and Q_B are the partition functions of the transition state and reactants, respectively. For the rate-determining transformation of the enzyme–substrate complex into the products the above expression can be written as

$$k = \kappa(T)\frac{k_B T}{h}\frac{Q_{\ddagger}}{Q_{ES}}\exp\left(-\frac{\Delta V^{\ddagger}_{ad}}{RT}\right) \qquad (8)$$

where the partition function of the reactants, Q_{ES}, should be similar to that of the transition state because they differ mostly in the extent of the C—H bond extension. Thus, the classical pre-exponential factor of Eq (8) can be written as $k_B T/h$, and has the numerical value of $6 \times 10^{12}\ s^{-1}$ at room temperature. As will be discussed further below, PCETs tend to be nonadiabatic and the actual value of the classical pre-exponential factor in Eq (8) does not affect the calculations presented in this work.

The vibrationally adiabatic path of Eq (6) with the modified Morse curves of Eq (5) and the electrophilicity index of Eq (4) gives the barrier necessary for rate constant calculations with Eqs (7) or (8). The tunnelling correction for that path is calculated with the semiclassical approximation of Truhlar and Garrett.[29] When H-bonds are present along the reaction coordinate, the reaction

Table 1. Bond lengths, bond dissociation energies, vibrational frequencies of the molecules and ionization potentials and electron affinities of the radicals employed in the calculation of the energy barriers[a]

	l_{eq} (Å)	D^0_{298} (kcal mol^{-1})	ω_e (cm^{-1})	I_P (eV)	E_A (eV)
C_6H_6	1.101	113.1	3062	8.32	1.096
H_2O	0.9575	119.0	3657	13.017	1.8277
$(CH_3)_3COOH$		84.2[b]			1.196[b]
HOOH	0.95	88.2	3608	11.35	1.078
$CH_2{=}CH\mathbf{C}H_2CH{=}CH_2$	1.110	76.6[c]	2982	7.25	

[a] Gas phase data; boldface letters indicate where the radical is centred after the bond to the hydrogen atom is broken; data from ref [35] and http://webbook.nist.gov or http://srdata.nist.gov/cccbdb/, except where noted.
[b] Ref.[36]
[c] Ref.[37]

path must be modified to include the presence of H-bonded complexes.

We have shown[17] that the Lippincott–Schroeder (LS) potential,[30] which gives an analytical relation between the H-bond binding energy ($D_{0,AHB}$) and the AB distance in the H-bonded complex ($l_{eq,AHB}$), can be included in the reaction path of ISM without loss of chemical insight. The H-bonded complex can be regarded as an incipient atom transfer, with a significant bond order between the hydrogen atom and the base ($n_{H\cdots B} > 0.1$). Therefore, when the rate-determining step is the conversion from precursor to successor complexes, we need only to consider the path connecting these complexes ($n_{H\cdots B} < n < 1-n_{H\cdots A}$). The energy barrier, in this case, is the difference between the maximum along this path (i.e., the transition state energy) and the minimum of the precursor complex.

In the breaking of a C—H bond in an enzyme-catalysed reaction, it is particularly important to assess the ability of the carbon atom to engage in a hydrogen bond with nitrogen or oxygen atoms. If we consider that H-bonding occurs when the distance between the proton and the acceptor atom is shorter than the sum of their van der Waals radii, a survey of crystal structures revealed that many systems meet this criterion for H-bonding between carbon acids and oxygen bases.[31] It is more likely to observe H-bonding to a carbon atom in a less polar environment, like in an enzyme, especially if the acceptor atom is charged or strongly polarized.[32] A remarkable example is the C—H···O contact between 1,2-diethylnylbenzene and a triphenylphosphine-water aggregate, $l_{eq,CHO} = 3.02$ Å, achieved through the polarization of the water molecule by its hydrogen bonding to two triphenylphosphine oxide molecules.[33] According to the LS potential, this should correspond to $D_{0,CHO} = 1.5$ kcal/mol. The (C—H···O) distance in the SLO/linoleic acid complex was estimated as $l_{CO} = 2.88$[4] or 2.95 Å,[10] and suggests an even stronger H-bond between the C(11) position of the substrate and SLO. Such a significant H-bond energy involving a CH bond has been explained by the strong electron withdrawal effect of the nearby Fe(III) ion.[3]

The rate calculations presented in this work require the data on Morse potentials and electronic properties of reactants and products presented in Table 1. In addition, the assessment of H-bonding in the reaction path requires information on the structure of the enzyme. With these data, the calculations take less than a second per temperature. An internet free-access site developed for ISM/scTST calculations[34] was used for all the rate calculations presented here. The supporting information includes the input files used in the internet calculations, as well as the most relevant data of the output files generated by such calculations.

RESULTS AND DISCUSSION

Uncatalysed H-atom abstraction from unsaturated fatty acids

H-atom transfers from unsaturated fatty acids by the cumylperoxyl radical in proprionitrile provide a good ground to clarify the mechanism of H-atom abstractions from C(11) of linoleic acid taking place in SLO. The peroxyl radical was first formed via a radical chain process and it was seen that its decay rate was accelerated in the presence of unsaturated fatty acids over an extended temperature range.[38] Scheme 1 shows the rate-determining step of the peroxyl radical decay in the presence of linoleic acid.

The ISM reaction coordinate for this H-atom transfer can be built from the C—H bond of 1,4-pentadiene to represent the equivalent C—H bond of linoleic acid, and with the O—H bond of *tert*-butyl hydroperoxide to represent the OH bond of cumyl hydroperoxide. The Morse parameters available for these CH and OH bonds are presented in Table 1. We were unable to find the O—H bond length and vibrational frequency of $(CH_3)_3COOH$, and replaced them by the data available for hydrogen peroxide. This is not expected to affect meaningfully our calculations because minor changes in bond lengths tend to be compensated by opposing changes in vibrational frequencies (or force constants).[19] In these calculations we also replaced the ionization potential of the *tert*-butyl peroxyl radical by that of the hydroperoxy radical, but this is immaterial because the calculation

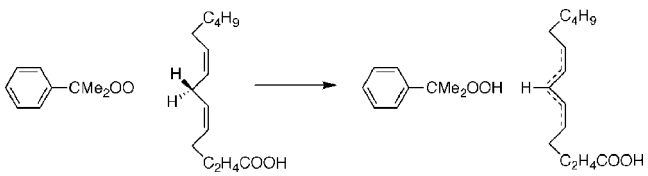

Scheme 1. H-atom abstraction at C(11) of linoleic acid by the cumylperoxyl radical

Table 2. Parameters employed in the ISM reaction coordinate of AH + B → A + HB H-atom transfers, and corresponding ISM/scTST rates

AH	HB	ΔG^0 kcal/mol	Reactant model	Product model	m	$D_{0(AHB)}$ kcal/mol	k_{ISM}	k_{exp}
$CPh(CH_3)_2OOH$	Linoleic a.	−11.6	HOOH	$(CH_2{=}CH)_2CH_2$	1.349	—	1.9×10^4	3.9[a]
SLO (linoleic a.)	SLO (13-HPOD)	−5.5	C_6H_6	H_2O	1	1.87; 1.87	5.4×10^{2}[b]	3.3×10^{2}[c]

[a] First-order rate constant, at −30 °C from Ref.[38]
[b] Nonadiabatic PCET calculated with a frequency factor of $3 \times 10^{11}\ s^{-1}$.
[c] At 25 °C, from Ref.[2]

of m for H-atom abstractions is governed[9] by the species of lowest I_P, which is the 1,4-pentadie-3-yl radical, and highest electron affinity, which is the *tert*-butyl peroxyl radical.

With the data discussed above, we obtained $\Delta V^0_{ad} = -11.6$ kcal/mol and $\Delta V^{\ddagger}_{ad} = 6.6$ kcal/mol. The experimental activation energy from measurements between −70 and −30 °C is 5.2 kcal/mol. The calculated barrier is in very good agreement with the activation energy because the tunnelling correction increases from 8 at −30 °C to 21 at −70 °C and reduces the temperature dependence of the rates. In fact, the activation energy obtained by the Arrhenius plot of the calculated rates is 4.6 kcal/mol. The tunnelling correction is probably overestimated at low temperatures because the experimental KIE increase from 6.0 ± 0.5 at −30 °C to 6.8 ± 0.6 at −60 °C, whereas the calculated values increase from 8 to 13, when the difference in frequency factors between the isotopes is neglected.[18,39] The agreement between calculated and experimental activation energies is within the average error of 0.96 kcal/mol previously obtained for 100 H-atom transfers in the gas phase and in solution.[9]

The H-atom transfer rate constant for this reaction must be calculated with Eq (7), which requires the calculation of partition functions of polyatomic species. We have shown that a typical value for pre-exponential factors of polyatomic reactions in the gas phase is $5 \times 10^8\ M^{-1}\ s^{-1}$.[9] However, the experimental data for this reaction in proprionitrile indicate that the pre-exponential factor is 2 orders of magnitude smaller than this. The sizes of the reactants in this bimolecular reaction are much larger than the sizes of typical reactants studied in the gas phase, and it is not surprising that the pre-exponential factor of a polyatomic gas phase reaction leads to an overestimate of the rate of H-abstraction of linoleic acid by the cumylperoxyl radical. Indeed, at −30 °C we calculate $6 \times 10^3\ M^{-1}\ s^{-1}$ and the experimental rate is $3.9\ M^{-1}\ s^{-1}$ (Table 2).

Soybean lipoxygenase-1

The formal H-atom abstraction of linoleic acid by SLO, Scheme 2, is a PCET, where the electron is transferred from the π-system of the linoleic acid (π_D) to the iron (Fe_A) and promotes the transfer of the proton from the C(11) carbon atom of linoleic acid to the oxygen atom of the Fe-bound OH ligand. The thermodynamic preference of SLO for a PCET pathway to the hydroperoxidation of linoleic acid rather than for a pure H-atom transfer has been duly appreciated.[2,40] Whereas a H-atom transfer is an adiabatic reaction, described by a smooth-potential energy surface with a strong interaction between the bonds breaking and forming at the transition state, a proper transition state and amenable to TST calculations, an outer-sphere electron transfer has a very small electronic coupling between the reactants, which is the source of its nonadiabaticity. The supposed nonadiabaticity of this PCET motivated its treatment with radiationless transitions theories based on the golden rule of quantum mechanics.[3–7] In adiabatic reactions, the overlap of vibronic wavefunctions gives rise to nuclear tunnelling and is incorporated as a pre-exponential correction to the TST rate expression, Eq (7), while retaining the classical frequency of the nuclear motion along the reaction coordinate, $\nu_N \approx k_B T/h$.

The nonadiabatic transfer of an electron over a large distance reduces its effective electronic frequency below ν_N,[41] and the effective electronic frequency becomes the reaction frequency.[42–44] In the case of SLO catalysis of the hydroperoxidation of linoleic acid, the π_D-Fe_A distance obtained from docking

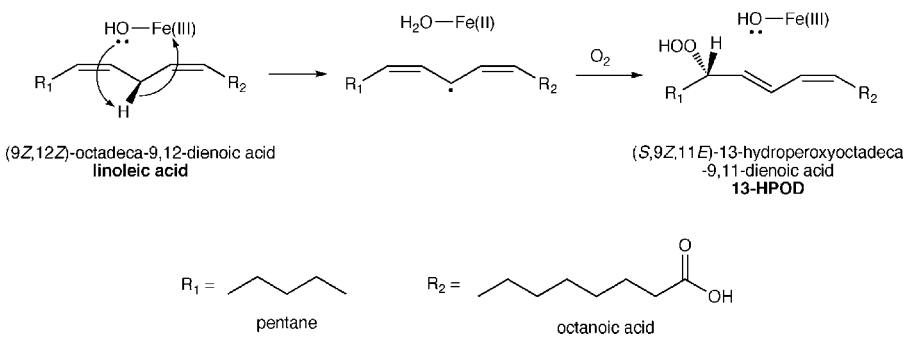

Scheme 2. PCET in the hydroperoxidation of linoleic acid catalysed by SLO

Journal of Physical Organic Chemistry

calculations is 5.69 Å and the Fe_A—O bond length is 1.86,[4] which lead to an edge-to-edge electron donor–acceptor distance of $\Delta r \approx 4$ Å. Edge-to-edge distance, rather than centre-to-centre distances, are employed for consistency with earlier work on electron transfer reactions.[41] Electron tunnelling through a square-potential barrier gives an effective electron frequency in the form

$$\nu = \nu_{el} \exp(-\beta_{el} \Delta r) \quad (9)$$

where $\nu_{el} = 10^{15}\,s^{-1}$ and the electronic decay coefficient can be expressed as[41,42]

$$\beta = -\frac{2}{\hbar}\sqrt{2m_e \frac{\Phi_0}{n_D^2}} \quad (10)$$

The energy of the electron in the donor ($\Phi_0 = 2.3$ V *vs.* NHE),[4] the refractive index of the intervening medium ($n_D = 1.33$ as in water) and the electron mass at rest (m_e) suffice to calculate the electron tunnelling decay coefficient of this system, $\beta_{el} = 2.0\,Å^{-1}$. This is only slightly higher than than measured for MTHF glass in other electron-transfer systems, 1.57–1.75 $Å^{-1}$.[45] With $\beta_{el} = 2.0\,Å^{-1}$ and $\Delta r \approx 4$ Å, we calculate a distance-dependent nonadiabatic factor of 3×10^{-4}. This factor multiplied by the frequency of the electron in the donor, $10^{15}\,s^{-1}$, gives a reaction frequency 20 times smaller than that of TST. This is the source of nonadiabaticity of this reaction, and we employ the nonadiabatic frequency factor of $3 \times 10^{11}\,s^{-1}$ in the place of the usual TST frequency, k_BT/h, for SLO catalysis.

As mentioned before, the crystallographic (CH···O) distance in the SLO/linoleic acid complex obtained by docking calculations[4] is virtually identical to that observed in the 1,2-diethylnylbenzene/triphenylphosphine-water aggregate and taken as evidence for the existence of (CH···O) hydrogen bonds.[31] According to the LS potential, $l_{CO} = 2.96$ Å gives $D_{0(CHO)} = 1.87$ kcal/mol and a H-bond stretching frequency of 167 cm^{-1}, consistent with the available data. The strong electron withdrawal effect of the nearby Fe(III) ion removes electron density away from the reaction coordinate, contributing both to the formation of a significant hydrogen bond and making m approach to unity.

ISM calculations also require Morse curve parameters to represent the OH and CH bonds involved in the reaction coordinate. Appropriate models are the O—H bond of H_2O and the C—H bond of benzene, because they typify the reactive bonds and give an adiabatic reaction energy of −5.5 kcal/mol, identical to the experimental ΔG^0.[4] Using the Morse curves of these bonds with the data in Table 1, the LS potential for a 1.87 kcal/mol (CH···O) H-bond, the nonadiabatic frequency factor $3 \times 10^{11}\,s^{-1}$, $m = 1$, and $\Delta V^0_{ad} = -5.5$ kcal/mol, we obtain a ISM/scTST rate of 540 s^{-1} and a KIE of 44 at 25 °C, in good agreement with the experimental values, $k_{cat} = 327 \pm 14\,s^{-1}$ and $k_H/k_D = 76$.[2] The large KIE results from a thin and high-energy barrier that leads to an extraordinary tunnelling correction of 100 at 25 °C. The barrier topography of this electron-coupled proton transfer is illustrated in Fig. 1.

This figure also represents the reaction path of the uncatalysed H-atom abstraction by the cumylperoxyl radical, which does not go through a H-bonded complex. In this case, barrier is wider and gives rise to normal tunnelling corrections and KIE. The comparison between the catalysed and uncatalysed reactions shows that the latter reaction is slightly more exothermic, but the presence of an H-bond in the reaction coordinate of the catalysed

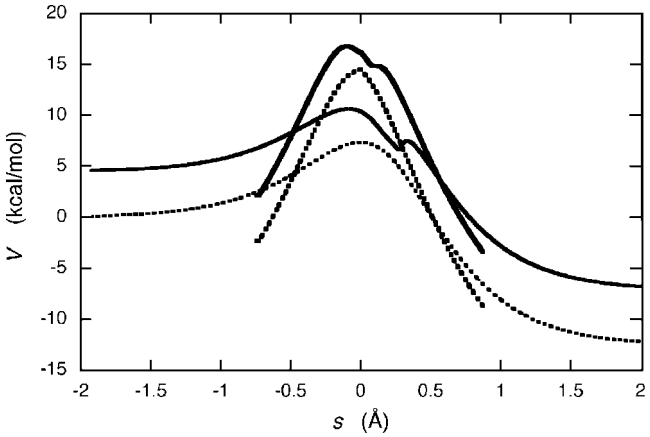

Figure 1. Classical and vibrationally adiabatic paths of ISM (dashed and solid lines, respectively) for the PCET of linoleic acid by SLO (thick lines), and for the hydrogen abstraction of 1,4-pentadiene by hydroperoxy radical (thin lines)

reaction is decisive in making it faster. Additionally, this H-bond leads to a thinner barrier, enhanced tunnelling and KIE, susceptibility to protein motion and selectivity.

It must be emphasized that a reasonably lower frequency factor and a stronger (CH···O) bond would bring the calculations into better agreement with the experimental data, but the objective of this work is not to fit parameters to the kinetic data. We are more interested in exploring the insights into enzyme catalysis that ISM/scTST calculation may offer, and the first conclusion from these results is that the TST view of catalysis is not incompatible with the large KIE observed at room temperature.

A detailed analysis of the temperature dependence of the rates in SLO catalysis must acknowledge the fact that, as the temperature increases, the protein expands and three factors contribute to decrease k_{cat}. The expansion of the protein increases the distance between the π-system of the linoleic acid and the iron reduces the refractive index of the intervening medium, and increases the distance between the CH and O atoms. The first two factors lead to a more pronounced nonadiabatic behaviour with an increase in temperature, which can be estimated from the thermal expansion of proteins and from the dependence of the refractive index on the temperature. We have made similar estimates for the reactive centre of photosynthetic bacteria using the linear thermal expansion of metmyoglobin, $115 \times 10^{-6}\,K^{-1}$,[46] and a temperature dependence of the refractive index typical of liquid solvents, $4.5 \times 10^{-4}\,K^{-1}$.[42] Taking the same coefficients for SLO, we calculate a 10% decrease in the pre-exponential factor as the temperature is increased from 25 to 50 °C. This is a relatively small change and will not be considered further. However, the increase in the distance between the CH and the O atoms with an increase in temperature decreases the H-bonding energy and has a significant impact on the rates. For example, an increase in l_{CO} of 0.001 Å per degree from 5 to 50 °C corresponds to a decrease in D_0 from 2.09 kcal/mol at 5 °C to 1.66 kcal/mol at 50 °C. As shown in Fig. 2, the H-bonding dependence on the temperature decreases the temperature dependence of the calculated reaction rates and brings them in good agreement with experimental data. The remarkable sensitivity of the PCET rate

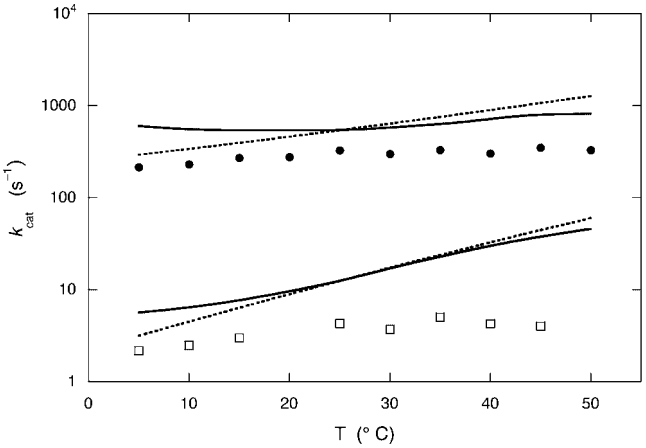

Figure 2. Temperature dependence of PCET in the hydroperoxidation of protio-linoleic acid (upper data) and deutero-linoleic acid (lower data) catalysed by SLO. The dashed lines represent the rates of ISM/scTST calculations with the reaction energy of -5.5 kcal mol^{-1}, and constant pre-exponential factors (3×10^{11} s^{-1}) and H-bond energies ($D_{0(CHO)} =$ 1.87 kcal/mol). The full lines represent similar calculations with expansion-dependent H-bond energies

to l_{CO} is mostly due to the sensitivity of H-tunnelling to this distance. Increasing l_{CO} by 0.025 Å reduces the tunnelling correction by 25%, and removing the H-bond from the reaction coordinate reduces the rate by a factor of 40 at 25 °C. This sensitivity enhances the role of protein dynamics in promoting, or suppressing, catalysis in this system. In fact, this sensitivity to the H-bond length can also be regarded as a dependence on the H-bond stretching frequency, because the two are interrelated by the LS potential. The H-bond frequency decreases from 184 cm^{-1} for $l_{CO} = 2.94$ Å to 167 cm^{-1} for $l_{CO} = 2.96$ Å, which is yet another example of how structure and dynamics are connected. The role of the H-bond frequency as the promoting mode of the enzymatic reaction is consistent with the simulations by Sutcliffe and co-workers, which identified a promoting vibration, with a frequency of 165 cm^{-1}, as the 'gating' motion from a CH bond of tryptamine to an oxygen atom of aromatic amine hydrogenase.

It is interesting to put these results in perspective referring to the data reported by Carey on the C═O stretching frequencies, bond lengths and H-bonding strengths of serine proteases. The hydrolysis of peptide bonds by this class of enzymes proceeds via an acyl enzyme intermediate, and the downshift in the carbonyl frequency by 54 cm^{-1} was correlated with an increase in the C═O bond length by 0.025 Å, an effective H-bonding strength of 14 kcal mol^{-1} and an increase in the deacylation rate by a factor of 10^4.[47] It must be noted that, in these systems, a longer C═O bond length corresponds to a shorter, and stronger, H-bond. These data reinforce our conclusions on the substantial acceleration produced by H-bonding when it occurs along the reaction coordinate of enzyme catalysis.

CONCLUSIONS

H-atom transfer rates in enzyme catalysis depend on the same parameters of H-atom transfers in the gas phase and in solution. The specificity of C—H bond breaking by SLO is the nonadiabaticity of the electron transfer associated with the cleavage of the C—H bond, and the presence of a C—H···O bond along the reaction coordinate. The nonadiabatic electron transfer associated with PCET reaction reduces the effective reaction frequency. This carries a penalty in terms of reaction rates, but is compensated by more favourable thermodynamics.

The presence of the H-bond leads to a thinner reaction barrier, enhanced H-tunnelling and a remarkable sensitivity to protein dynamics. Tunnelling corrections at room temperature usually range from 2 to 15, but in enzyme catalysis through H-bonded reactive bonds the tunnelling corrections may increase the rates by three orders of magnitude. The rates, KIEs and temperature dependences of the hydroperoxidation of linoleic acid catalysed by SLO have been shown previously to be very sensitive to the distance between donor and acceptor atoms and to be influenced by protein dynamics.[2–8] ISM/scTST calculations assign the nearly temperature-independent rates and KIE to temperature-dependent reaction barriers due to changes in H-bond energy.

Acknowledgements

We thank Fundação para a Ciência e a Tecnologia (Portugal) e FEDER for financial support; project no. POCI/QUI/55505/2004. MB thanks the financial support by FCT through grant BPD/22070/2005.

REFERENCES

[1] A. Kohen, J. P. Klinman, *Acc. Chem. Res.* **1998**, *31*, 397–404.
[2] M. J. Knapp, K. Rickert, J. P. Klinman, *J. Am. Chem. Soc.* **2002**, *124*, 3865–3874.
[3] W. Siebrand, Z. Smedarchina, *J. Phys. Chem. B* **2004**, *108*, 4185–4195.
[4] E. Hatcher, A. V. Soudackov, S. Hammes-Schiffer, *J. Am. Chem. Soc.* **2004**, *126*, 5763–5775.
[5] S. Hammes-Schiffer, *Acc. Chem. Res.* **2006**, *39*, 93–100.
[6] E. Hatcher, A. V. Soudackov, S. Hammes-Schiffer, *J. Am. Chem. Soc.* **2007**, *129*, 187–196.
[7] M. P. Meyer, J. P. Klinman, *Chem. Phys.* **2005**, *319*, 283–296.
[8] J. R. E. T. Pineda, S. D. Schwartz, *Philos. Trans. R. Soc. B* **2006**, *361*, 1433–1438.
[9] L. G. Arnaut, A. A. C. C. Pais, S. J. Formosinho, M. Barroso, *J. Am. Chem. Soc.* **2003**, *125*, 5236–5246.
[10] G. Tresadern, J. P. McNamara, M. Mohr, H. Wang, N. A. Burton, I. H. Hillier, *Chem. Phys. Lett.* **2002**, *358*, 489–494.
[11] M. H. M. Olsson, P. E. M. Siegbahn, A. Warshel, *J. Am. Chem. Soc.* **2004**, *126*, 2820–2828.
[12] M. H. M. Olsson, J. Mavri, A. Warshel, *Philos. Trans. R. Soc. B* **2006**, *361*, 1417–1432.
[13] M. Garcia-Viloca, J. Gao, M. Karplus, D. G. Truhlar, *Science* **2004**, *303*, 186–195.
[14] J. Pu, J. Gao, D. G. Truhlar, *Chem. Rev.* **2006**, *106*, 3140–3169.
[15] Y. Cha, C. J. Murray, J. P. Klinman, *Science* **1989**, *243*, 1325–1330.
[16] K. M. Doll, B. R. Bender, R. G. Finke, *J. Am. Chem. Soc.* **2003**, *125*, 10877–10884.
[17] M. Barroso, L. G. Arnaut, S. J. Formosinho, *ChemPhysChem.* **2005**, *6*, 363–371.
[18] M. Barroso, L. G. Arnaut, S. J. Formosinho, *J. Phys. Chem. A* **2007**, *111*, 591–602.
[19] L. G. Arnaut, S. J. Formosinho, *Chem. Eur. J.* **2007**, *13*, 8018–8028.
[20] L. G. Arnaut, S. J. Formosinho, *Chem. Eur. J. in press.*
[21] R. G. Parr, L. v. Szentpály, S. Liu, *J. Am. Chem. Soc.* **1999**, *121*, 1922–1924.
[22] H. S. Johnston, C. Parr, *J. Am. Chem. Soc.* **1963**, *85*, 2544–2551.
[23] L. Pauling, *J. Am. Chem. Soc.* **1947**, *69*, 542–553.
[24] A. J. C. Varandas, F. B. Brown, C. A. Mead, D. G. Truhlar, B. C. Garrett, *J. Chem. Phys.* **1987**, *86*, 6258–6269.

[25] L. G. Arnaut, S. J. Formosinho, M. Barroso, *J. Mol. Struct.* **2006**, *786*, 207–214.
[26] L. Arnaut, S. Formosinho, H. Burrows, *Chemical Kinetics*, Elsevier, Amsterdam, **2007**.
[27] E. B. Wilson, Jr. *J. Chem. Phys.* **1939**, *7*, 1047–1052.
[28] S. Galsstone, K. J. Laidler, H. Eyring, *The Theory of Rate Processes*, McGraw-Hill, New York, **1941**.
[29] B. C. Garrett, D. G. Truhlar, *J. Phys. Chem.* **1979**, *83*, 2921–2926.
[30] E. R. Lippincott, R. Schroeder, *J. Chem. Phys.* **1955**, *23*, 1099–1106.
[31] R. Taylor, O. Kennard, *J. Am. Chem. Soc.* **1982**, *104*, 5063–5070.
[32] S. Scheiner, T. Kar, *J. Phys. Chem. B* **2005**, *109*, 3681–3689.
[33] B. M. Kariuki, K. D. M. Harris, D. Philp, J. M. A. Robinson, *J. Am. Chem. Soc.* **1997**, *119*, 12679–12680.
[34] L. G. Arnaut, M. Barroso, D. Oliveira, *Intersecting/Interacting State Model*, **2006**, http://www.ism.qui.uc.pt:8180/ism/
[35] CRC *Handbook of Chemistry and Physics*, 81st Edition, D.R. Lide, Ed; CRC Press, Boca Raton, FL, **2000**.
[36] S. J. Blanksby, T. M. Ramond, G. E. Davico, M. R. Nimlos, S. Kato, V. M. Bierbaum, W. C. Lineberger, G. B. Ellison, M. Okumura, *J. Am. Chem. Soc.* **2001**, *123*, 9585–9596.
[37] K. B. Clark, P. N. Culshaw, D. Griller, F. P. Lossing, J. A. M. Simoes, J. C. Walton, *J. Org. Chem.* **1991**, *56*, 5535–5539.
[38] H. Kitaguchi, K. Ohkubo, S. Ogo, S. Fukuzumi, *Chem. Commun.* **2006**, 979–981.
[39] H.-H. Limbach, J. M. Lopez, A. Kohen, *Philos. Trans. R. Soc. B* **2006**, *361*, 1399–1415.
[40] N. Lehnert, E. I. Solomon, *J. Biol. Inorg. Chem.* **2003**, *8*, 294–305.
[41] S. J. Formosinho, L. G. Arnaut, R. Fausto, *Prog. React. Kinet.* **1998**, *23*, 1–90.
[42] L. G. Arnaut, S. J. Formosinho, *J. Photochem. Photobiol. A: Chem.* **1997**, *111*, 111–138.
[43] C. Serpa, L. G. Arnaut, S. J. Formosinho, K. R. Naqvi, *Photochem. Photobiol. Sci.* **2003**, *2*, 616–623.
[44] C. Serpa, P. J. S. Gomes, L. G. Arnaut, S. J. Formosinho, J. Seixas de Melo, J. Pina, *Chem. Eur. J.* **2006**, *12*, 5014–5023.
[45] O. S. Wenger, B. S. Leigh, R. M. Villahermosa, H. B. Gray, J. R. Winkler, *Science* **2005**, *307*, 99–102.
[46] H. Frauenfelder, H. Hartmann, M. Karplus, I. D. Kuntz, Jr., J. Kuriyan, F. Parak, G. A. Petsko, D. Ringe, R. F. Tilton, Jr., M. L. Connolly, N. Max, *Biochemistry* **1987**, *26*, 254–261.
[47] P. R. Carey, *Chem. Rev.* **2006**, *106*, 3043–3054.

